Journal of Soil Science and Plant Nutrition (2025) 25:5494–5507
https://doi.org/10.1007/s42729-025-02472-2

ORIGINAL PAPER

Microplastics Influence Phosphate Adsorption in Volcanic Ash Soil

Jonathan Suazo-Hernández[1,2,3] · Lizethly Cáceres-Jensen[4] · Hector Pesenti[5] · Fabio Corradini[6] · María de la Luz Mora[1] · Nanthi Bolan[7,8] · Pablo Cornejo[9,10] · Binoy Sarkar[3]

Received: 3 November 2024 / Accepted: 6 May 2025 / Published online: 29 May 2025

Abstract

Purpose: There is a debate whether microplastic particles released into soils can modify phosphorus bioavailability by altering the soil surface properties. Here, we aim to explore the impact of polyethylene microplastics (PE–MPs) on the adsorption–desorption of inorganic phosphate anions (P) on a volcanic ash soil (VAS). Methods: Batch P adsorption-desorption experiments were conducted in a Chilean VAS with and without 1% (w/w) PE-MPs addition taking P concentrations (KH_2PO_4 dissolved in 0.01 mol L^{-1} NaCl background solution) 0.02–6.47 mmol L^{-1}, solid (g):liquid (mL) ratio 1:40, and at a pH range of 4.5 to 10.5 at 20 ± 1 °C temperature. The VAS and VAS/PE–MPs systems were characterized and kinetic and isotherm adsorption data were modelled to predict mechanisms. Results: The Elovich model described the kinetics P adsorption data on VAS with and without 1% PE–MPs ($r^2 \geq 0.985$ and $\chi^2 \leq 12$). Adsorption isotherms fitted well to the Freundlich model ($r^2 \geq 0.994$ and $\chi^2 \leq 6.39$), indicating a high heterogeneous surface for both systems. The Freundlich model indicated an increase in P adsorption capacity from 49.55 (mmol kg^{-1}) (L $mmol^{-1})^{1/n}$ for VAS to 54.66 (mmol kg^{-1}) (L $mmol^{-1}$)1/n for VAS + 1% PE–MPs. Desorption of P was higher in the VAS + 1% PE–MPs system compared to VAS alone. For both systems, solution pH showed no significant changes in P adsorption on VAS. Scanning electron microscopy–energy dispersive X–ray spectroscopy and Fourier transform infrared spectroscopy results showed that P was bound to PE–MPs through a weak van der Waals force and/or pore–filling mechanism. Conclusion: This study demonstrated that PE–MPs in VAS could modify surfaces available for P adsorption and act as a carrier to enhance P mobility.

Keywords Emerging contaminants · Plant nutrients · Plastic pollution · Soil phosphorus · Eutrophication

✉ Binoy Sarkar
binoy.sarkar@unisa.edu.au

[1] Center of Plant, Soil Interaction and Natural Resources Biotechnology, Scientific and Biotechnological Bioresource Nucleus (BIOREN-UFRO), Universidad de La Frontera, Avenida Francisco Salazar 01145, Temuco, Chile

[2] Facultad de Medicina Veterinaria y Agronomía, Universidad de Las Américas, Sede Concepción, Chile

[3] Future Industries Institute, University of South Australia, Mawson Lakes SA 5095, Australia

[4] Physical & Analytical Chemistry Laboratory (PachemLab), Departamento de Química, Facultad de Ciencias Básicas, Universidad Metropolitana de Ciencias de La Educación, Santiago, Chile

[5] Núcleo de Investigación en Bioprocesos y Materiales Avanzados, Facultad de Ingeniería, Universidad Católica de Temuco, 4780000 Temuco, Chile

[6] Instituto de Investigaciones Agropecuarias, INIA La Platina, Casilla 439, Correo 3, Santiago, Chile

[7] School of Agriculture and Environment, The University of Western Australia, Perth, WA 6009, Australia

[8] The UWA Institute of Agriculture, The University of Western Australia, Perth, WA 6009, Australia

[9] Centro de Estudios Avanzados en Fruticultura (CEAF), Rengo, 2940000 Santiago, Chile

[10] Centro Tecnológico de Suelos y Cultivos (CTSyC), Facultad de Ciencias Agrarias, Universidad de Talca, 3460000 Talca, Chile

1 Introduction

Over 320 million tons of plastics are produced worldwide annually, mostly ending up in the environment (Cressey 2016). Once in the environment, plastic debris, due to weathering and degradation processes via solar radiation, high temperature, wind, dispersion in water, and grinding with sand and gravels, break down into microplastics (MPs) (Andrady 2011; Duan et al. 2021). According to the National Oceanic and Atmospheric Administration (NOAA), MPs are plastic particles with sizes/diameters < 5 mm (Malla-Pradhan et al. 2022) that exhibit a high specific surface area, amorphous structure, hydrophobicity, and high porosity (Wang et al. 2020). The amount of MPs in soils is currently between 4 and 23 times higher than in oceans (Horton et al. 2017). Coming in contact with soil, MPs can accumulate and modify the chemical, physical, and biological properties of the soil, including the water retention capacity, aggregation behavior, pH, and microbial and enzymatic activities (Pinto-Poblete et al. 2022; Vithanage et al. 2021; Zhang et al. 2021; Zhao et al. 2021). MPs can also affect the transport of nutrients/pollutants and organic compounds from soil to surface water and groundwater, and cause changes in nutrient/pollutant bioavailability (Dong et al. 2020). Accordingly, the need to understand the behavior of MPs in the soil in relation to nutrient and pollutant bioavailability is immense.

Adsorption–desorption interactions with soil particle surfaces significantly govern the bioavailability of nutrients/pollutants in the soil (Jing et al. 2024). Therefore, many studies explored the phenomena of nutrient/pollutant bioavailability in the soil to determine the environmental risk of MPs (Hu et al. 2020; Li et al. 2020; Ma et al. 2022). Furthermore, the bioavailable fraction of nutrients and pollutants in the terrestrial system depends not only on the total amount of elements present in the environment but also on their solubility, which is affected by the physicochemical properties of the soil (Sarkar et al. 2021; Zhang et al. 2020a). In particular, the adsorption of nutrients and pollutants on MPs and subsequent desorption can alter nutrient/pollutant bioavailability, resulting in risks for the microbiota, plants, and other environmental receptors (Wang et al. 2022).

Previous studies have evaluated the effect of MPs on the adsorption of organic and inorganic cationic pollutants in soils with comparatively less emphasis on anionic pollutants (Li et al. 2023; Wang et al. 2020; Zhang et al. 2020a). The surface charge, hydrophobicity, and surface area values of MPs could directly influence the adsorption–desorption of nutrients and pollutants in soils. For example, Zhang et al. (2020a) determined that in an Alfisol, cations such as Cd^{2+} could be adsorbed on the surface of polyethylene (PE) MPs. This was mainly associated with MPs having a negative surface charge, favoring an electrostatic attraction with the cationic form of the element. On the other hand, only a few studies have investigated the effect of MPs on the adsorption–desorption processes of anionic nutrients/pollutants such as borate, selenate, sulfate, nitrate, nitrite, and phosphate (P) in soils. The interaction between MPs and anionic elemental species in soils is largely unknown (Abbasi 2024). Particularly, volcanic ash soils (VAS; e.g., Andisol and Ultisol) cover an area of 0.84% of the world's land surface, and VAS are essential to support the global food demand (Dahlgren et al. 2004). VAS are present in countries such as Chile, Colombia, Indonesia, Taiwan, New Zealand, and Japan (Minasny et al. 2021). VAS have low bioavailability of P, which is due to the high fixation capacity of P on amorphous mineral components of these soils (Borie et al. 2019; Escudey et al 2001). The P accumulated in VAS mostly exists in organic forms through the formation of Fe/Al-organic matter-P complexes (Borie and Zunino 1983). A recent study by Riveros et al. (2024) reported that a dose of 3% low-density polyethylene and polyamide MPs adversely affected the chemical and biological properties, including P availability, nitrate (NO_3^-) and nitrite (NO_2^-) concentrations, and acid phosphatase and β-glucosidase activities, in a VAS, which could impact the nutrient cycling process of the soil. P is an essential macronutrient which is needed for an optimal plant growth. Therefore, studies concerning P–MP–VAS interactions are critical to evaluate the effect of the emerging MP pollutants on the functionality and health of soil, which ultimately determines the soil's productivity.

To date, only a limited number of studies have evaluated the interaction of MPs–P anions in soils, and these studies reported that P was adsorbed on MPs through a weak van der Waals force (Li et al. 2021), which was responsible for the increase in P bioavailability in the soil (Li and Liu 2022). However, no research on MPs was carried out to investigate MP–modified P bioavailability in VAS. This gap in the literature underscores the novelty of the present study. This study particularly aims to: i) evaluate the impact of PE–MPs on the interaction of P as dihydrogen phosphate ($H_2PO_4^-$) anions and surface reaction of VAS, and ii) provide evidence about the impact of MPs on P bioavailability in VAS agroecosystems. It was hypothesized that the presence of PE–MPs would change P bioavailability in a VAS by changing the physico–chemical characteristics of the soil, such as solution pH, specific surface area, elemental composition and/or surface functional groups. This research is important to ensure soil health, and especially that of VAS, because the findings could enable a deeper understanding of the impact of MPs on the biogeochemical

cycles of nutrients, and help to devolop future strategies to minimize the adverse environmental impact of MPs.

2 Materials and Methods

2.1 Chemicals

All reagents (KH_2PO_4, NaOH, HCl, and NaCl) used in this study were of analytical grade (Merck). All the chemicals were used as received, and aqueous stock solutions of chemicals were prepared in double–distilled water (conductivity ≤ 1 µS cm^{-1}).

2.2 Soil Sample

A VAS belonging to the Santa Barbara series located in southern Chile (36° 50′ S; 113 71° 55′ W) was collected at 0–20 cm depth, naturally air-dried at room temperature for 72 h and sieved (< 2 mm). This VAS was previously described by Suazo-Hernández et al. (2021).

2.3 Polyethylene–MP Sample

Polyethylene (PE) pellets were acquired from BO Packaging company, Chile. PE–MPs were prepared using the PE pellets by freezing in liquid nitrogen followed by crushing in a grain crusher. The crushed material was sieved into a particle size range of 100–250 µm using a Standard ISO-3310.1 sieve (Cisa Cedacería Industrial, Spain). The density of PE–MPs measured with a pycnometer was 0.85 g cm^{-3}.

2.4 Characterization of VAS and MP Samples

Soil pH was determined in 1:2.5 soil:double–distilled water ratio. Organic matter (OM) content was determined after wet digestion of sample using a modified Walkley–Black procedure. Total P was extracted from the soil sample by alkaline oxidation with NaBrO (Tabatabai and Bremner 1970) and the supernatant was filtered and subsequently the concentration of total P was determined using a Rayleigh – 2601 UV spectrophotometer (BRAIC Co. Ltd., Beijing, China) at 880 nm wavelength. The total nitrogen (TN) content of VAS was measured using an elemental analyser (Euro EA3000, EuroVector, Italy). Cation exchange capacity (CEC) of the soil was estimated by extracting the exchangeable cations (Na, K, Mg, and Ca) using $NH_4CH_3CO_2$ (1 M, pH 7.0). The cation concentrations in clear filtrate were measured using atomic absorption spectroscopy (AAS, Thermo Fisher ICE-3500 AAS, USA) (Sadzawka et al. 2006). Exchangeable Al was extracted with KCl (1 M) and measured using AAS. Effective cation exchange capacity (ECEC) was calculated as the sum of exchangeable Al plus the CEC.

The zeta potential (ZP) of PE–MPs and VAS was determined as a suspension of 20 mg particles in 10 mL NaCl solution (0.01 mol L^{-1}) using a Nano ZS apparatus (Malvern Instruments, Worcestershire, UK) at 20 °C. The isoelectric point (IEP) was obtained from the graph of ZP versus pH. The specific surface area of VAS, PE–MPs, and VAS + 1% + PE–MPs were obtained using the Brunauer, Emmett, and Teller nitrogen adsorption/desorption technique with a Quantachrome Nova 1000e physisorption analyzer (Boynton Beach, FL, USA). The Barrett–Joyner–Halenda model was used to determine the average pore volume and size.

The morphological characteristics of the surface of pristine PE–MPs were acquired by a scanning transmission electron microscope (STEM) using a STEM SU–3500 instrument (Hitachi, Tokyo, Japan). The scanning electron microscope (SEM) images obtained were analyzed to calculate the average length of the particles using the ImageJ program (version 1.50i, National Institute of Health, Bethesda, MD, USA). The elemental composition of PE–MPs was analyzed by SEM coupled to an energy dispersive X–ray (SEM–EDX) spectrometer before and after the adsorption of P in VAS + 1% PE–MP system using a QUANTAX 100 Advanced BRUKER EDX microanalysis detector (Bruker Corporation, USA). The PE–MPs were isolated from the VAS + 1% PE–MPs adsorption isotherm system having the highest initial P concentration (6.47 mmol L^{-1}) by centrifugation at 12,000 rpm for 10 min. The PE–MP samples isolated from the soil were deposited onto formvar/carbon–coated grids and inspected under a high vacuum mode**.**

The PE–MPs were characterized by X–ray diffraction (XRD) before and after isolation from the soil following P adsorption in VAS + 1% PE–MP system. The XRD measurement was taken using a Shimadzu XRD–6000 powder diffractometer (Columbia, Maryland, USA) at 1.5418 Å with CuKα radiation in the 2θ region from 10 to 80°.

The Fourier transform infrared (FT–IR) spectra of VAS and PE–MPs were recorded before P adsorption and for PE–MPs after their isolation from the soil following P adsorption in the VAS + 1% PE–MP system. FT–IR analysis of samples was performed with a Cary 630 spectrometer (Agilent Technologies, Santa Clara, CA, USA). The transmission spectra were realized with 4 cm^{-1} resolution, and the operating wavelength ranged from 4,000 to 600 cm^{-1} at atmospheric pressure and 20 °C temperature.

2.5 Batch Adsorption–Desorption Studies

Batch adsorption studies were conducted to investigate the removal capacity of P by adsorption onto VAS and VAS + 1% PE–MP systems in centrifuge tubes at 20 °C following the methodology suggested by Shirkhorshidi et al. (2023). It involved an air-drying of the soil at room temperatura for 72 h before the adsorption tests. The experimental adsorption conditions used in these studies are summarized in Table 1.

Table 1 Parameters evaluated in the batch adsorption experiments

Parameters	Weight MPs	Initial pH	Kinetics	Isotherms
Agitation time (min)	1,440	1,440	0–1,440	1,440
MPs dose (%)	0–2	1	1	1
Adsorbent dose (g)	0.5	0.5	0.5	0.5
Initial P concentration (mmol L^{-1})	6.47	6.47	6.47	0.02–6.47
NaCl concentration (mol L^{-1})	0.01	0.01	0.01	0.01
pH solution	5.5 ± 0.2	4.5–10.5 ± 0.2	5.5 ± 0.2	5.5 ± 0.2
Volume of adsorbate (mL)	20	20	20	20
Shaking speed (rpm)	200	200	200	200

The samples from experiments examining the effect of MPs doses, initial solution pH, adsorption kinetics, and adsorption isotherm were centrifuged at 12,000 rpm for 10 min and filtered through 0.22 µm pore size syringe filters. When studying the effect of initial solution pH ($pH_{Initial}$) on P adsorption, the final solution pH (pH_{Final}) was also determined after P adsorption.

The P concentration in the filtered solution was determined using the molybdate–blue method (Murphy and Riley 1962) with a Rayleigh–2601 UV spectrophotometer. The P amount adsorbed (q_e, mmol kg^{-1}) was determined by Eq. 1.

$$q_e = \frac{(C_0 - C_t)V}{m} \quad (1)$$

where, C_o and C_t are the initial and time t, or the equilibrium concentrations of P (mmol L^{-1}), respectively, m is the mass of VAS used (kg), and V is the volume (L).

At the completion of the adsorption isotherm experiments, desorption were conducted immediately by taking the P-adsorbed solids with the highest initial P concentration. The desorption of P from the VAS and VAS + 1% PE–MP systems was carried out by applying four successive extractions with 20 mL of double–distilled water into the tubes and shaking at 200 rpm for 1440 min at 20 ± 1 °C. After shaking, the solution was filtered through a 0.22 µm pore size syringe filter to determine the P concentration. The P desorption (%) was determined from the adsorbed concentration of P on soil systems, and the concentration of P desorbed into the aqueous solution, using Eq. 2.

$$\text{Desorption (\%)} = \frac{\text{P desorbed}}{\text{P adsorbed}} x100\% \quad (2)$$

2.6 Adsorption Kinetics and Isotherm Models and Data Analysis

The adsorption kinetic and isotherm models used in this study are summarized in Supplementary Information (Tables 1S and 2S). The Elovich, pseudo–second–order (PSO), and pseudo–first–order (PFO) kinetic models, and Langmuir and Freundlich isotherm models were tested through non–linear fitting. Additionally, the intraparticle diffusion (IPD) kinetic model was tested in a step–wise linear form. These models provide different adsorption perspectives and are complementary regarding the P adsorption process in VAS, allowing to predict the key underlying mechanisms (Dunne et al. 2021). It is however important to recognize that no single model can describe the complexity of the interaction between P in VAS and VAS-MP systems.

Table 2 Selected properties of the volcanic ash soil used in this study

Parameter	Volcanic ash soil
pH (in H_2O)	5.40 ± 0.02
Organic matter (%)	14.1 ± 0.07
Total N (%)	0.74 ± 0.03
Total P (mg kg^{-1})	1,76641 ± 27.01
K ($cmol_{(+)}$ kg^{-1})	0.89 ± 0.04
Na ($cmol_{(+)}$ kg^{-1})	0.09 ± 0.01
Ca ($cmol_{(+)}$ kg^{-1})	6.45 ± 0.33
Mg ($cmol_{(+)}$ kg^{-1})	1.34 ± 0.09
Al ($cmol_{(+)}$ kg^{-1})	0.08 ± 0.01
ECEC ($cmol_{(+)}$ kg^{-1})*	8.85 ± 0.48
Isoelectric point (IEP)	3.2

*Efective cation exchange capacity

All experiments were performed in triplicate in this study. A blank sample without the VAS was also included. Results presented in the paper are the means ± standard error. The data obtained from both kinetic and isotherm studies were evaluated through the chi–squared (χ^2) and coefficient of determination (r^2) parameters. To evaluate the effect of PE–MPs on the P adsorption–desorption processes in VAS, a Student's t-test was applied when statistical assumptions were met (normal distribution and homoscedasticity). The statistical analysis of the adsorption data was realized to express the difference between mean values. Figures were drawn with the Origin 2019b software (OriginLab, USA).

3 Results

3.1 Characterization of Volcanic Ash Soil

The VAS presented an OM content of around 14%, a moderate acidity (pH = 5.40) and high levels of Ca and Mg, and low Al, K, and Na levels (Table 2). Furthermore, VAS exhibited an average concentration of total P (1,766 mg kg^{-1}) and total N (0.74%), and an IEP value of 3.2. The mineral composition of the VAS was dominated by allophane, kaolinite and vermiculite (Escudey et al. 2001).

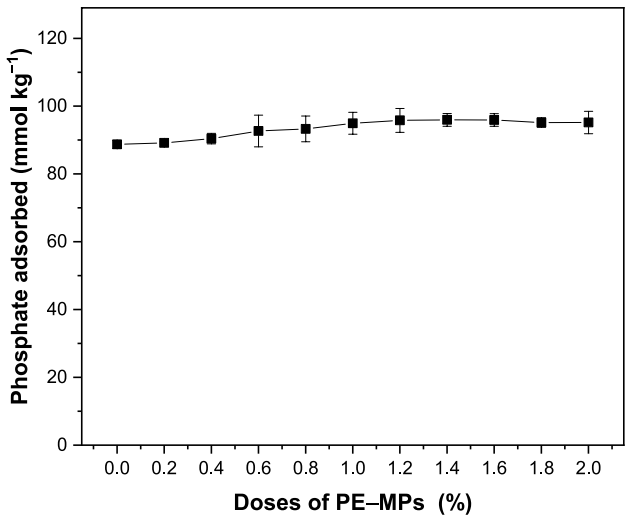

Fig. 1 Effect of polyethylene microplastics (PE–MPs) on the adsorption of phosphate anions on a volcanic ash soil at an initial phosphate concentration of 6.47 mmol L^{-1} in 0.01 mol L^{-1} NaCl; initial pH 5.5 ± 0.2; reaction volume 20 mL. Error bars indicate standard error; $n = 3$

3.2 Effect of PE–MP Doses on P Adsorption

Figure 1 shows the effect of increasing PE–MP doses from 0 to 2% on the adsorption of P (initial P concentration = 6.47 mmol L^{-1}) on VAS. The increase in the dose of PE–MPs resulted in a slight increase in the adsorption of P on the VAS sample. In particular, the VAS without PE–MPs showed an adsorption of P equivalent to 88.73 mmol kg^{-1} (initial P concentration = 258.8 mmol kg^{-1}, 34.82%). When the PE–MP dose increased to 2%, the adsorption of P was 95.19 mmol kg^{-1} (37%). We chose a dose of 1% PE–MPs from the above results for subsequent adsorption–desorption studies.

3.3 Effect of Initial Solution pH on P Adsorption

The pH had a direct effect on the ionization of surface functional groups of the VAS and VAS + 1% PE–MP systems, and on the speciation of P, which consequently would play a vital role in the P adsorption behavior. Figure 2a shows that as the pH value was increased, there was a decrease in P adsorption on VAS and VAS + 1% PE–MP systems. The presence of 1% PE–MPs increased the adsorption of P by VAS in the entire pH range under the study. In addition, at higher pH, the difference in P adsorption between VAS and VAS + 1% PE–MPs decreased because the interaction between PE–MPs and P became less favorable due to the increasing negative surface charge of both PE–MPs and VAS (Fig. 2a). The release of OH^- groups into the solution (i.e., increase in solution pH or positive ΔpH) following P adsorption were higher for VAS alone system than VAS + 1% PE–MP system (Fig. 2b), which could be attributed to an increased OH^- ligand exchange mechanism for P adsorption occurring in the former system compared to the latter.

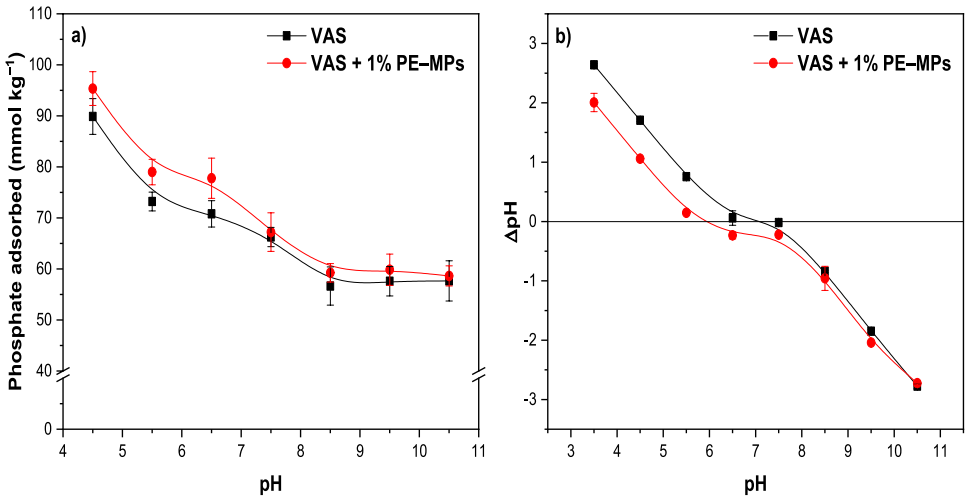

Fig. 2 a) Effect of initial solution pH on the adsorption of phosphate anions in the absence and presence of 1% polyethylene microplastics (PE–MPs) on a volcanic ash soil (VAS), and b) variation of pH (ΔpH: pH_{Final}–$pH_{Initial}$) before and after adsorption of P at different initial pH values and at initial P concentration 6.47 mmol L^{-1} in 0.01 mol L^{-1} NaCl, and reaction volume 20 mL. Error bars indicate standard error; $n = 3$

3.4 P Adsorption Kinetic Studies

The kinetic adsorption of P on VAS and VAS + 1% PE–MP systems were realized at 20 °C at an initial solution pH of 5.5 over 0 to 1,440 min (Figs. 3a). The P adsorption efficiency during the first 10 min was very low, reaching around 57.34 mmol kg^{-1} (22.20%), and 63.43 mmol kg^{-1} (24.55%) for VAS and VAS + 1% PE–MPs, respectively. The curves became linear after 60 min, resulting in a P adsorption of 74.44 mmol kg^{-1} (28.81%) and 76.23 mmol kg^{-1} (29.51%) for VAS and VAS + 1% PE–MP system, respectively. Meanwhile, at 720 min, the adsorption reached 90.59 mmol kg^{-1} (35.41%) and 92.66 mmol kg^{-1} (35.86%) for VAS and VAS + 1% PE–MP system, respectively. This showed that a long contact time significantly influenced the adsorption of P in VAS. After 720 min, no significant difference was observed in P adsorption, indicating that both the VAS and VAS + 1% PE–MP systems reached an adsorption equilibrium at around 720 min.

Experimental data were fitted to the PFO, PSO, Elovich, and IPD kinetic models (Figs. 3b–d). The kinetic model parameters obtained are provided in Table 3. The models allowed us to predict the kinetic rates and mechanisms of P adsorption on the studied systems. Based on high values of r^2 and low values of χ^2 obtained, the Elovich model ($r^2 \geq 0.985$ and $\chi^2 \leq 12$) provided a better fitting of the experimental data for VAS and VAS + 1% PE–MPs than the PFO and PSO models (Table 3). The IPD model (Weber–Morris) was also applied to analyze the transport mechanism of P using the experimental data. The IPD model describes the penetration of adsorbate into the interior of a substrate (Rusmin et al. 2015). The values of the IPD model parameters, k_{int} and C, were obtained from the slope and intercept of the graph q_t versus $t^{1/2}$. According to the graph shown in Fig. 3d, the adsorption of P on VAS and VAS + 1% PE–MPs occurred in three steps. The first part of the curve, with very high r^2 values (≥ 0.966), represented a uniform distribution of P on the external surface of the soil (film diffusion). The second step was dominated by IPD, which suggested that the P gradually diffused into the aggregates (intraparticle diffusion), and the last part of the curve (equilibrium phase or interaction) reflected the adsorption equilibrium, where the adsorption slowed down due to the saturation of adsorption sites of VAS.

3.5 P Adsorption Isotherm Studies

The isotherm adsorption of P on the VAS and VAS + 1% PE–MPs systems are shown in Fig. 4a. In every case, the adsorption isotherm was L–type, indicating that the VAS in the presence or absence of 1% PE–MPs had a high affinity for P. In particular, the curves for both systems did not reach a plateau. The experimental data were fitted non–linearly to the Langmuir and Freundlich models (Fig. 4b–c,

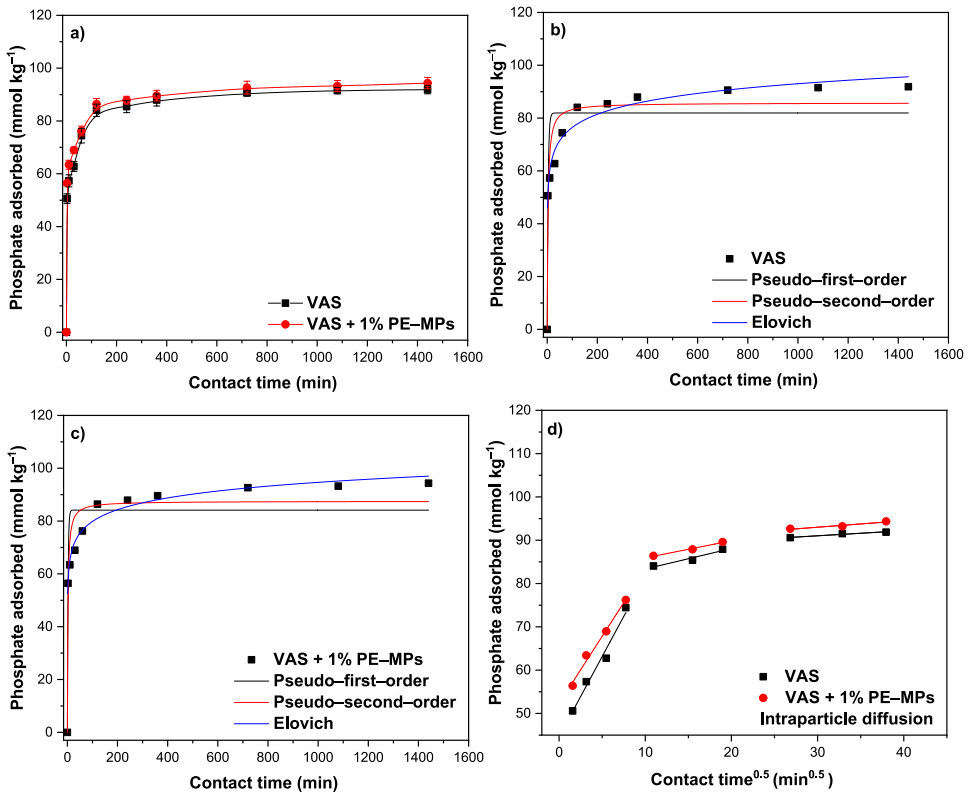

Fig. 3 a) Phosphate adsorption kinetics at initial pH 5.5 ± 0.2 in 0.01 mol L^{-1} NaCl in the absence and presence of 1% polyethylene microplastics (PE–MPs) on a volcanic ash soil (VAS), b) phosphate adsorption kinetics on a VAS modelled by pseudo–first–order, pseudo–second–order and Elovich model, c) phosphate adsorption kinetics on a VAS in the presence of 1% PE–MPs modelled by pseudo–first–order, pseudo–second–order and Elovich models, and d) phosphate adsorption kinetics on a VAS in the absence and presence of 1% PE–MPs modelled by intraparticle diffusion model. Error bars indicate standard error; $n = 3$

Table 3 Parameters of pseudo–first–order, pseudo–second–order, Elovich and intraparticle diffusion models obtained from adsorption kinetics of phosphate (± standard error) on volcanic ash soil (VAS) in the absence and presence 1% polyethylene microplastics (PE–MPs) a pH 5.5 ± 0.1

Kinetic parameters	VAS	VAS + 1% PE–MPs
q_{exp} (mmol kg^{-1})	91.88 ± 5.40	94.35 ± 6.42
q_{exp} (%)	35.57	37.32
	Pseudo–first–order	
q_e (mmol kg^{-1})	81.94 ± 4.02	84.16 ± 3.54
k_1 (× 10^{-2} min^{-1})	27.41 ± 10.48	38.91 ± 13.33
r^2	0.823	0.858
χ^2	143	203
	Pseudo–second–order	
q_e (mmol kg^{-1})	85.78 ± 3.17	87.53 ± 2.84
k_2 (× 10^{-3} kg $mmol^{-1}$ min^{-1})	3.80 ± 1.34	5.38 ± 1.83
h (mmol kg^{-1} min^{-1})	27.96 ± 0.01	41.22 ± 0.01
r^2	0.912	0.926
χ^2	71	62
	Elovich	
α (mmol kg^{-1} min^{-1})	2,987.67 ± 265.24	15,814.12 ± 697.55
β (× 10^{-2} kg $mmol^{-1}$)	13.91 ± 1.06	15.54 ± 1.00
r^2	0.985	0.991
χ^2	12	7
	Intraparticle diffusion	
K_{int1} (mmol kg^{-1} $min^{-0.5}$)	3.70 ± 0.40	3.10 ± 0.24
C_1 (mmol kg^{-1})	44.69 ± 2.00	52.35 ± 1.20
r^2	0.966	0.983
K_{int2} (mmol kg^{-1} $min^{-0.5}$)	0.47 ± 0.12	0.39 ± 0.04
C_2 (mmol kg^{-1})	78.64 ± 1.82	82.00 ± 0.69
r^2	0.884	0.944
K_{int3} (mmol kg^{-1} $min^{-0.5}$)	87.52 ± 0.84	88.49 ± 1.21
C_3 (mmol kg^{-1})	0.12 ± 0.02	0.15 ± 0.04
r^2	0.910	0.886

and Table 4). According to the high values of r^2 and low values of χ^2 obtained, the Freundlich model ($r^2 \geq 0.994$ and $\chi^2 \leq 6.39$) better described the P adsorption data on VAS and VAS + 1% PE–MP systems than the Langmuir model.

3.6 P Desorption Studies

The degree of desorption varied with the binding strength between the adsorbent and the adsorbate. Figure 5 shows the P desorption results of VAS systems after being extracted four times (successively) with double–distilled water. The P desorption (%) from VAS was 70.83%, and on VAS + 1% PE–MPs system was 72.40% after four successive cycles. In other words, VAS + 1% PE–MPs desorbed 1.02 times greater amount of P than the VAS alone.

3.7 SEM–EDX Analysis

SEM–EDX results revealed that the pristine PE–MPs were mainly dominated by C (Fig. 6a). After the adsorption of P on VAS + 1% PE–MP system, the signal of C in the isolated PE–MP sample was maintained alongside the appearance of new signals for Na, O, Si, K, Cl and P (Fig. 6b). These results indicated that a certain amount of P remained bound to the PE–MPs following the adsorption experiments.

3.8 XRD Analysis

The XRD patterns of the PE–MPs pre– and after the P adsorption showed the characteristic reflections of the PE–MPs, which were observed at 2Θ values of 21.1° and 23.4° (Fig. S1) (Randhawa 2023). After the adsorption of P, the PE–MPs isolated from the soil showed XRD reflections at similar 2Θ values stated above. Therefore, the XRD results suggested that the crystallinity of PE–MPs did not change before and after P adsorption in the soil.

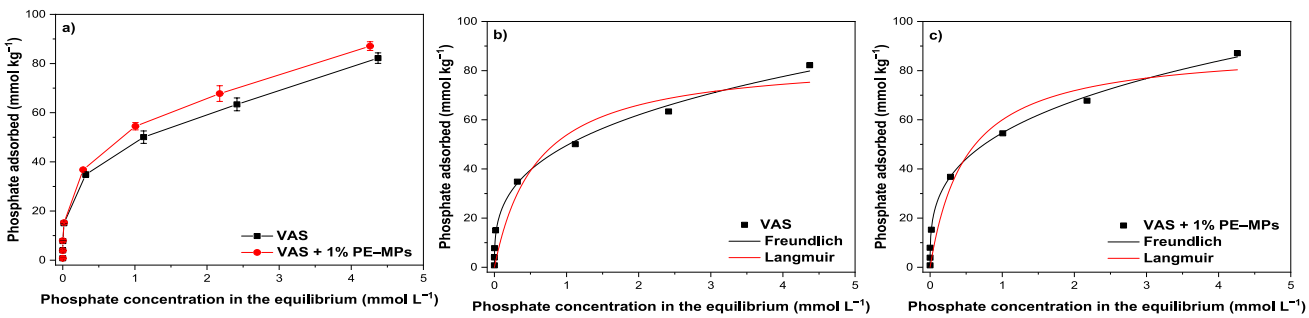

Fig. 4 a) Phosphate adsorption isotherms at initial pH 5.5 ± 0.2 in 0.01 mmol L^{-1} NaCl in the absence and presence of 1% polyethylene microplastics (PE–MPs) on a volcanic ash soil (VAS), b) phosphate adsorption isotherms on a VAS modelled by the Langmuir and Freundlich models, and c) phosphate adsorption isotherm on a VAS in the presence of 1% PE–MPs modelled by the Langmuir and Freundlich models. Error bars indicate standard error; $n = 3$

Table 4 Langmuir and Freundlich parameters (± standard error) for phosphate adsorption isotherms at pH 5.5 ± 0.2 in the absence and presence of 1% polyethylene microplastics (PE–MPs) on a volcanic ash soil (VAS)

System	Langmuir				Freundlich			
	K_L (L mmol^{-1})	q_{max} (mmol kg^{-1})	r^2	χ^2	K_F (mmol kg^{-1}) (L mmol $^{-1}$)$^{1/n}$	n	r^2	χ^2
VAS	1.70 ± 0.80	85.41 ± 10.68	0.943	61.74	49.55 ± 1.28	3.09 ± 0.19	0.994	6.39
VAS + 1% PE–MPs	2.02 ± 0.86	89.71 ± 9.77	0.952	58.79	54.66 ± 1.11	3.23 ± 0.17	0.996	5.45

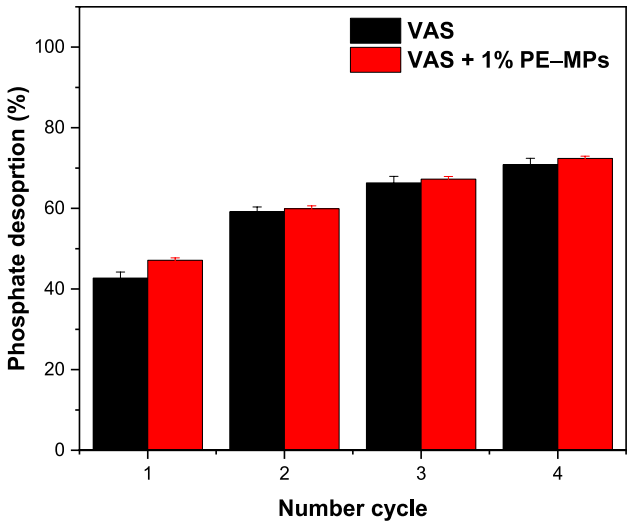

Fig. 5 Phosphate desorption (%) obtained from volcanic ash soil (VAS) soil in the absence and presence of 1% polyethylene microplastics (PE–MPs) using 20 mL of double–distilled water, and shaking at 200 rpm for 1,440 min at 20 ± 1 °C. Error bars indicate standard error; $n = 3$

3.9 FT–IR Analysis

FT–IR spectroscopy was used to characterize functional group changes on PE–MPs surfaces pre– and after P adsorption (Fig. 7). The FT–IR spectra of the pristine PE–MPs showed two bands at 2,919 cm^{-1} and 2,851 cm^{-1}, which indicated an asymmetric and symmetric vibration of CH_2, respectively (Kovács et al. 2021; Zhang et al. 2020b). The FT–IR spectra also showed two absorption bands at 1,463 cm^{-1} and 721 cm^{-1}, corresponding to the C–H bending deformation and C–C rocking vibration, respectively (Kovács et al. 2021; Zhang et al. 2020b). After the adsorption of P, the FT–IR spectra of the PE–MPs isolated from VAS showed the above adsorption bands and a new band at 962 cm^{-1}, which did not appear in the FT–IR spectra of VAS (Fig. S2). The new band corresponded to a symmetric bending vibration of P–O bonds (Gu et al. 2021).

4 Discussion

We evaluated the influence of PE–MPs on P adsorption–desorption processes on a typical VAS (Table 1) (Cartes et al. 2009), which is of importance since P is one of the most limiting nutrients for agricultural activities in this type of soils (Pizarro et al. 2017; Vistoso et al. 2012). We found that 1% PE–MPs slightly increased the P adsorption capacity of the soil (Fig. 4) and also increased P desorption (Fig. 5). Anion adsorption on VAS was studied extensively in the past (Gonzalez-Rodriguez and Fernandez-Marcos 2021; Vistoso et al. 2012) but not often in the presence of MPs. This study obtained a maximum P adsorption value in the VAS (85.41 mmol kg^{-1}) similar to those already reported (Vistoso et al. 2012, 2009). PE–MPs were also shown to adsorb anions such as $H_2PO_4^-$ (Khan and Hodson 2024), $Cr_2O_7^{2-}$ (Zhang et al. 2020b), and $HAsO_4^-$ and AsO_2^- (Nguyen et al. 2023). Soil comprises various inorganic and organic components, including minerals (e.g., silicates, aluminosilicates, iron oxides, and aluminium oxides) and OM. In particular, VAS contains amorphous minerals such as allophane, imogolite, and ferrihydrite, which have a strong anion adsorption capacity, especially P anions (Escudey et al. 2004; Pizarro et al. 2017). The main mechanism proposed for P adsorption on VAS has been ligand exchange via OH^- groups that are exposed at the colloidal amorphous mineral surface in this type of soils (Vistoso et al. 2012).

The PE–MPs we used had a highly hydrophobic surface, an irregular morphology (size between 250 µm and 50 µm; with an average length of 145.39 µm) (Fig. S3a and S3b), a high specific surface area (4.81 m^2 g^{-1}), high porosity (0.005 cm^3 g^{-1}) (Table 3S) and a net negative surface charge at pH 5.5 (Fig. S4) at which the adsorption studies were performed. These characteristics might partly explain why the P adsorption capacity of VAS was altered in the presence of 1% PE–MPs. We found a slight but insignificant ($p > 0.05$) influence of the PE–MP dose on the P adsorption by VAS. Particularly, the increase in PE–MP dose led to a slightly upward trend in the P adsorption capacity of the soil. The addition of 2% PE–MPs provided the most notable increase in P adsorption. This increase might be associated with the affinity of PE–MPs for P anions.

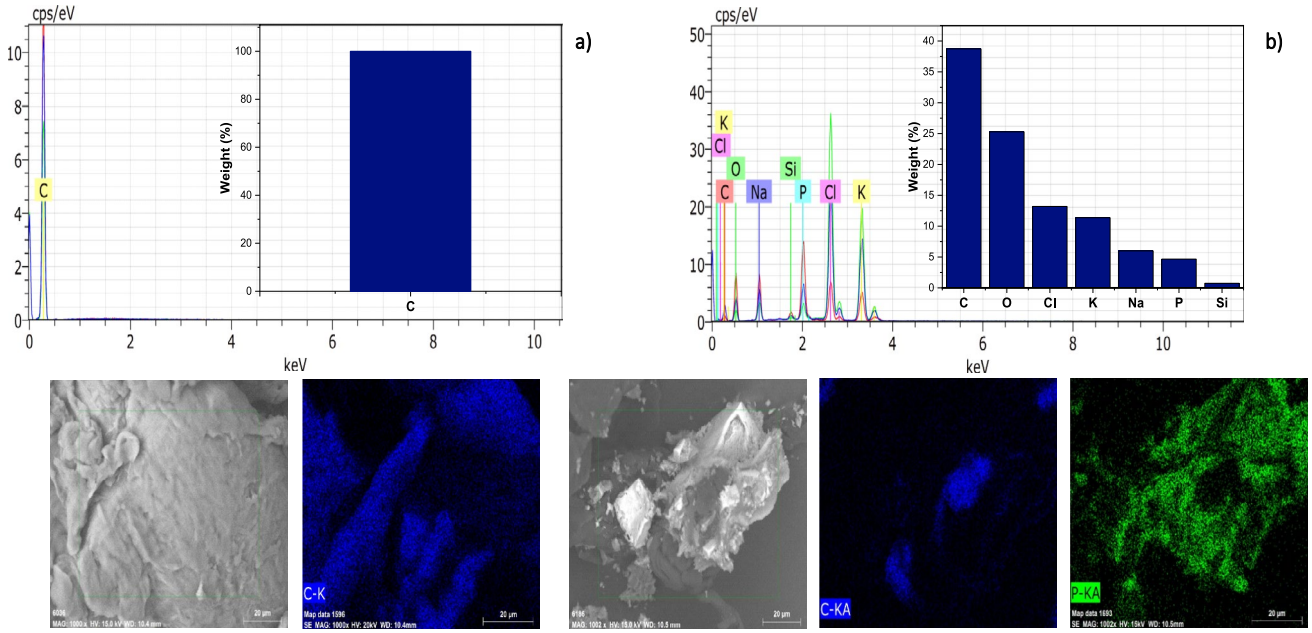

Fig. 6 SEM–EDX spectra of polyethylene microplastics isolated from a volcanic ash soil; a) without phosphate, and b) after adsorption of phosphate, at initial pH 5.5 ± 0.2 in 0.01 mol L^{-1} NaCl, and reaction volume 20 mL

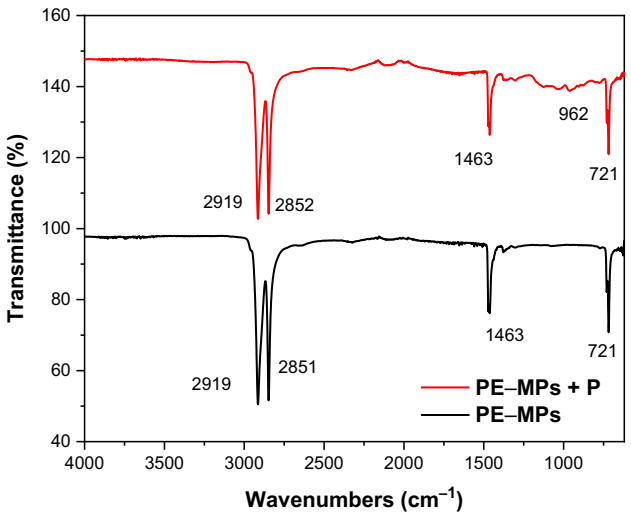

Fig. 7 FT–IR spectra of polyethylene microplastics (PE–MPs) before and after the adsorption procedure in 6.47 mmol L^{-1} phosphate (P) at initial pH 5.5 ± 0.2 in 0.01 mol L^{-1} NaCl, and reaction volume 20 mL

Similar to our results, Shi et al. (2022) reported an increased adsorption of P on soil collected from sweet potato field in Ezhou, China, following an addition of 1% and 5% of PE–MPs. The pH of the solution could exert a noticeable influence on the adsorption of oxyanions on VAS and VAS + 1% PE–MP systems (Cáceres-Jensen et al. 2009; Cáceres et al. 2010; Hiradate and Uchida 2004; Pigna and Violante 2003). Ligand exchange reaction between the adsorbent's surface functional groups and $H_2PO_4^-$ could be promoted at an acidic solution pH (Suazo-Hernández et al. 2021). In contrast, P adsorption could decrease at an alkaline pH due to electrostatic repulsion followed by a decreased ligand exchange (Suazo-Hernández et al. 2021). Our study found that P adsorption was slightly higher on VAS + 1% PE–MP than VAS alone at acidic pH, and the adsorption did not remarkably change at alkaline pH. The small difference in P adsorption capacity observed at acidic pH between the VAS and VAS + 1% PE–MP systems could be attributed to the favorable electrostatic interaction between P anions and PE–MPs, possibly due to the presence of MPs agglomerates at the soil surface (Khan and Hodson 2024; Luo et al. 2024). At very high pH values, the surface of PE–MPs was negatively charged, and the interaction between PE–MPs and P anions could be hampered by electrostatic repulsion force (Zhang et al. 2020b). High pH values could cause electrostatic repulsion between MP particles, increasing their dispersion. This would decrease the presence of PE–MPs in soil agglomerates, and consequently decrease the amount of adsorption sites for P (Luo et al. 2024). At acidic pH, a positive and higher value of ΔpH was obtained for P adsorption on VAS + 1% PE–MP than on VAS alone, suggesting that ligand exchange reaction was more favorable for the interaction of $H_2PO_4^-$ with surface functional groups of VAS than between $H_2PO_4^-$ and VAS + 1% PE–MPs. At an alkaline pH, negative and similar values of ΔpH in both VAS and VAS + 1% PE–MP systems were obtained, probably due to a decreasing trend of ligand exchange mechanism

between $H_2PO_4^-$ and VAS as a consequence of the presense of PE–MPs (Chen et al. 2024).

The kinetic data of P adsorption on VAS and VAS + 1% PE–MPs were fitted to the PFO, PSO, IPD and Elovich models. The Elovich model describes a chemisorption process (strong binding force) on a heterogeneous surface and establishes no interaction among the adsorbed species (Fizir et al. 2024; Suazo-Hernández et al. 2022). The fitness of the experimental data of this study to the Elovich model suggested that the dominant P adsorption mechanism on VAS and VAS + 1% PE–MPs was through the formation of a chemical bond between P and binding sites of the adsorbents.

The values of the Elovich model parameters α and β varied as a function of the presence of PE–MPs (Table 3). The value of β increased from 13.91×10^{-2} kg mmol^{-1} for VAS to 15.54×10^{-2} kg mmol^{-1} for VAS + 1% PE–MP system, indicating that PE–MPs added some P adsorption sites in the VAS matrix. At the same time, the presence of PE–MPs caused an increase in the value of α from 2,987.67 to 15,814.12 mmol kg^{-1} min^{-1} for VAS and VAS + 1% PE–MPs, respectively. Irrespective of the presence and absence of PE–MPs, the values of α were higher than β, suggesting a greater feasibility of the P adsorption process than desorption (Suazo-Hernández et al. 2021). A good fitness of the Elovich model for P adsorption on VAS was also reported in previous studies (Suazo-Hernández et al. 2023; Suazo-Hernández et al. 2021; Vistoso et al. 2009). The Elovich model, however, was unable to identify the diffusion mechanism, which was elucidated by using the IPD model. If the adsorption rate is controlled by intraparticle diffusion, the graph in Fig. 3d must be straight and pass through the origin (0,0) (Caceres Jensen et al. 2019). Otherwise, the adsorption would be controlled by multiple processes (Caceres Jensen et al. 2019; Mezenner and Bensmaili 2009). In the current study, the graph did not pass through the origin; therefore, IPD was not the only rate controlling step in P adsorption on VAS and VAS + 1% PE–MPs (Caceres Jensen et al. 2019). From the IPD model, three stages were distinguished for P adsorption in both systems.

The values of K_{int} for VAS and VAS + 1% PE–MPs showed a tendency of $K_{int3} > K_{int1} > K_{int2}$ (Table 3). This might be due to P adsorption occurring rapidly on the surface, favoring a saturation of the adsorption sites. This saturation would cause P to penetrate into the adsorbent's surface, rapidly entering the pores and leaving free sites on the surface of the adsorbent (Zhao et al. 2022). Nevertheless, the film diffusion rate constant (K_{int1}) for the VAS system was 1.19 times higher than for the VAS + 1% PE–MP system (Table 3). This indicated that P transport through the liquid film was slower in the presence of PE–MPs. The low slopes of the intraparticle diffusion segments (k_{int2}) in both systems, 0.47 mmol kg^{-1} min$^{-0.5}$ for VAS and 0.39 mmol kg^{-1} min$^{-0.5}$ for VAS + 1% PE–MPs, indicated a slow diffusion rate in the adsorbent pores, regardless of the presence of PE–MPs (Costigan et al. 2022).

Previous studies found that the Langmuir and Freundlich isotherm models could describe P adsorption behaviors in volcanic soils (Suazo-Hernández et al. 2023; Suazo-Hernández et al. 2021). The present study showed that without and with 1% PE–MPs, the Freundlich isotherm model fitted better to the experimental data for P adsorption on VAS than the Langmuir model (Table 4). This meant that the adsorption of P on VAS without and with 1% PE–MPs occurred in multilayers on a heterogeneous surface (Kalam et al. 2021). These results are consistent with those obtained from the good fitting of the kinetic adsorption data to the Elovich model. Similar findings were reported by Khan and Hodson (2024) for P adsorption in some arable soils in the UK without and with PE–MPs.

The P adsorption isotherm for VAS and VAS + 1% PE–MPs yielded high values of the adsorption intensity (n = 3.09 and 3.23, respectively) when fitting to the Freundlich model (Table 4). The P adsorption capacity, as expressed by the K_F values, was 54.65 (mmol kg^{-1}) (L mmol^{-1})$^{1/n}$ for VAS + 1% PE–MPs versus 49.55 (mmol kg^{-1}) (L mmol $^{-1}$)$^{1/n}$ for VAS. In other words, the relative P adsorption capacity was 1.10 times higher for VAS + 1% PE–MPs than VAS. In addition, this study showed that although the addition of 1% PE–MPs decreased the specific surface area and pore volume of VAS (Table S3), the VAS + 1% PE–MP system practically had the same adsorption capacity to P than VAS alone.

The slightly increased adsorption of P on VAS could primarily be related to the specific surface area, porosity, and –CH_2 groups of PE–MPs (Table S3), because P ($H_2PO_4^{2-}$) could be adsorbed on this material through pore filling mechanism and van der Waals forces (Brennecke et al. 2016). This hypothesis was also supported in an earlier study by Chen et al. (2019), who reported that tri–n–butyl phosphate and tris(2–chloroethyl) phosphate were adsorbed on PE–MPs by pore–filling mechanism. Shao et al. (2023) reported that the adsorption of $Cr_2O_7^{2-}$ on PE–MPs also occurred through the micropore filling effect and van der Waals forces.

The SEM–EDX (Fig. 6) and FT–IR (Fig. 7) results confirmed the presence of P on the surface of PE–MPs isolated from the soil after adsorption of P on VAS + 1% PE–MPs system, indicating that the effect of PE–MPs was not just a simple dilution effect, but a direct interaction of the surface of MPs with P anions. On the contrary, no changes were observed in the XRD pattern of PE–MPs before and after P adsorption on VAS + 1% PE–MPs system (Fig. 1S), which indicated that the adsorption of a small amount of P over a short period of time did not affect the crystallinity of PE–MPs. These results indicated that a weak binding force

between PE–MPs and P anions could have also contributed to P adsorption in the VAS + 1% PE MPs system. Therefore, chemical adsorption was not the only mechanism of P adsorption on VAS + 1% PE–MPs. It could be speculated that pore–filling and/or physical interaction mechanisms might have dominated the adsorption of P by PE–MPs. In contrast, a chemical adsorption mechanism dominated for P adsorption to original VAS particles.

Another notable result of this study was that the percentage of P desorption from VAS increased, but insignificantly ($p > 0.05$), when 1% PE–MPs were added to the system. These results indicated that P adsorbed on PE–MPs was washed away when H_2O was used as the desorbing agent. The results revealed that MPs occupied the specific adsorption sites of VAS for P (Mai et al. 2023), and again suggested that P was bound weakly to VAS + 1% PE–MPs than VAS without PE–MPs. Similar to the results of the current study, Li et al. (2021) reported that P adsorption on PE–MPs occurred through van der Waals forces (physical interaction). Khan and Hodson (2024) also found a high level of P desorption from high–density (HD) PE–MPs and HDPE–MPs + soil systems, which the authors attributed to a weak van der Waals interaction force between HDPE–MPs and P.

Several studies showed that MPs could modify the chemical and physical properties of soils (e.g., aggregate stability, bulk density, porosity, water holding capacity, and pH) (de Souza MacHado et al. 2018; Ding et al. 2022; Jiang et al. 2017), and the availability of elements (Ma et al. 2022; Zhou et al. 2020). However, studies on VAS, which are characterized by having a high water–holding capacity, and OM content, acidic pH, non-crystalline minerals (allophane, ferrihydrite, and imogolite), and Al-humus complexes, are minimal (Cook et al. 2022; Corradini et al. 2021). One of the very few studies conducted on Chilean terrestrial systems reported that the most common MPs are PE, polypropylene, acrylates, polyurethane, varnish, nitrile rubber, and polystyrene, which can reach soils mainly through the disposal of sewage sludge (Corradini et al. 2019). On that basis, we used a PE type MPs to approximate its effect of P adsorption–desorption in VAS, with the limitation of laboratory studies, what could occur in the real system. The results of the adsorption–desorption studies, for the first time, confirmed that the addition of 1% PE–MPs slightly increased P adsorption on VAS and P desorption capacity from the soil too, increasing the release of P into the soil solution. This consequently could increase the mobility of P towards groundwater, posing additional problems for the environment. This also means that when PE–MPs and P coexist in a VAS, P availability for plants and soil biota could increase slightly. The results of this study thus may have long-reaching implications for agriculture, particularly in VAS, where nutrient management is crucial to maintain the soil quality and health. Considering the exponential increase of MPs concentrations in agroecosystems and their possible impacts on soil functions (Baeza et al. 2020), future studies must focus on determining the influence of PE–MPs as well as other types of MPs on the environmental behavior of plant nutrients such as K, Cu, Zn, N, S, Mo, and Se, and to unravel the fate and transformation of MPs in VAS.

5 Conclusions

Experimental results in the batch systems showed that increasing the polyethylene microplastics (PE–MPs) dose slightly increased the adsorption of phosphate (P) on the volcanic ash soil (VAS). The addition of 1% PE–MPs to VAS slightly increased P desorption too with respect to VAS alone. The results of the spectroscopic analyses showed that P might bind to PE–MPs through physical interaction (van der Waals forces) and/or pore–filling mechanisms. The overall results revealed that 1% PE–MPs could potentially increase the P bioavailability in the VAS. In addition, 1% PE–MPs changed the soil physical properties, which could alter the soil health and hydraulic conductivity, and these warrant further investigations. This study forms the basis for researching how MPs could affect nutrient bioavailability in VAS in Chile and other countries and deliver useful information to assess the impact of MPs in the functionality of terrestrial systems.

Supplementary Information The online version contains supplementary material available at https://doi.org/10.1007/s42729-025-02472-2.

Acknowledgements Special thanks to Technological Bioresource Nucleus (BIOREN-UFRO) and Soil and Plant Laboratory. This work was partially funded by the Research Directorate of Universidad de La Frontera.

Author contributions **Jonathan Suazo-Hernández:** Conceptualization; Investigation; Funding acquisition; Formal analysis; Data curation; Writing – review & editing; Writing – original draft. **Lizethly Cáceres-Jensen:** Methodology; Visualization; Writing – original draft. **Hector Pesenti**: Software; Investigation. **Fabio Corradini:** Conceptualization; Methodology. **María de la Luz Mora:** Funding acquisition; Resources; Supervision. **Binoy Sarkar:** Conceptualization; Investigation; Validation; Supervision; Writing – review & editing. **Nanthi Bolan:** Investigation; Writing – review & editing. **Pablo Cornejo:** Conceptualization; Investigation; Writing – original draft.

Funding Open Access funding enabled and organized by CAUL and its Member Institutions. This study was supported by the Agencia Nacional de Investigación y Desarrollo de Chile (ANID) (grant number FONDECYT Postdoctoral Grant N° 3230179).

Data Availability Data will be made available on request.

Declarations

Competing Interests The authors María de la Luz Mora, Lizethly Cáceres-Jensen, and Jonathan Suazo-Hernández are Associate Editors for Journal of Soil Science and Plant Nutrition (JSSPN) and the peer-review process for this article was independently handled by another member of the journal editorial board.

References

Abbasi S (2024) Uncovering the intricate relationship between plant nutrients and microplastics in agroecosystems. Chemosphere 346:140604. https://doi.org/10.1016/j.chemosphere.2023.140604

Andrady AL (2011) Microplastics in the marine environment. Mar Pollut Bull 62:1596–1605. https://doi.org/10.1016/j.marpolbul.2011.05.030

Baeza C, Cifuentes C, González P, Araneda A, Barra R (2020) Experimental Exposure of Lumbricus terrestris to Microplastics. Water Air Soil Pollut 231:1–10. https://doi.org/10.1007/s11270-020-04673-0

Borie F, Zunino H (1983) Organic matter-phosphorus associations as a sink in P-fixation processes in allophanic soils of Chile. Soil Biol Biochem 15:599–603. https://doi.org/10.1016/0038-0717(83)90056-1

Borie F, Aguilera P, Castillo C, Valentine A, Seguel A, Barea JM, Cornejo P (2019) Revisiting the Nature of Phosphorus Pools in Chilean Volcanic Soils as a Basis for Arbuscular Mycorrhizal Management in Plant P Acquisition. J Soil Sci Plant Nutr 19:390–401. https://doi.org/10.1007/s42729-019-00041-y

Brennecke D, Duarte B, Paiva F, Caçador I, Canning-Clode J (2016) Microplastics as vector for heavy metal contamination from the marine environment. Estuar Coast Shelf Sci 178:189–195. https://doi.org/10.1016/j.ecss.2015.12.003

Cáceres-Jensen L, Gan J, Báez M, Fuentes R, Escudey M (2009) Adsorption of glyphosate on variable-charge volcanic ash–derived soils. J Environ Qual 38:1449–1457. https://doi.org/10.2134/jeq2008.0146

Cáceres L, Fuentes R, Escudey M, Fuentes E, Báez ME (2010) Metsulfuron-methyl sorption/desorption behavior on volcanic ash–derived soils. Effect of Phosphate and pH. J Agric Food Chem 58:6864–6869. https://doi.org/10.1021/jf904191z

Caceres Jensen L, Neira-albornoz A, Escudey M (2019) Herbicides Mechanisms Involved in the Sorption Kinetic of Ionisable and Non Ionisable Herbicides: Impact of Physical/Chemical Properties of Soils and Experimental Conditions. In: Kinetic Modeling for Environmental Systems. pp 1–15

Cartes P, Jara AA, Demanet R, de la Mora M, L, (2009) Urease Activity and Nitrogen Mineralization Kinetics As Affected By Temperature and Urea Input Rate in Southern Chilean Andisols. Rev La Cienc Del Suelo y Nutr Veg 9:69–82. https://doi.org/10.4067/s0718-27912009000100006

Chen S, Tan Z, Qi Y, Ouyang C (2019) Sorption of tri-n-butyl phosphate and tris(2-chloroethyl) phosphate on polyethylene and polyvinyl chloride microplastics in seawater. Mar Pollut Bull 149:110490. https://doi.org/10.1016/j.marpolbul.2019.110490

Chen Y, Li Y, Liang X, Lu S, Ren J, Zhang Y, Han Z, Gao B, Sun K (2024) Effects of microplastics on soil carbon pool and terrestrial plant performance. Carbon Res 3:37. https://doi.org/10.1007/s44246-024-00124-1

Cook D, Malinauskaite L, Davíðsdóttir B (2022) Peering into the fire – An exploration of volcanic ecosystem services. Ecosyst Serv 55:101435. https://doi.org/10.1016/j.ecoser.2022.101435

Corradini F, Meza P, Eguiluz R, Casado F, Huerta-Lwanga E, Geissen V (2019) Evidence of microplastic accumulation in agricultural soils from sewage sludge disposal. Sci Total Environ 671:411–420. https://doi.org/10.1016/j.scitotenv.2019.03.368

Corradini F, Casado F, Leiva V, Huerta-Lwanga E, Geissen V (2021) Microplastics occurrence and frequency in soils under different land uses on a regional scale. Sci Total Environ 752:141917. https://doi.org/10.1016/j.scitotenv.2020.141917

Costigan EM, Oehler MA, MacRae JD (2022) Phosphorus recovery from recirculating aquaculture systems: Adsorption kinetics and mechanism. J Water Process Eng 49:102992. https://doi.org/10.1016/j.jwpe.2022.102992

Cressey D (2016) The Plastic Ocean. Nature 536:263–265

Dahlgren RA, Saigusa M, Ugolini FC (2004) The Nature, Properties and Management of Volcanic Soils. Adv Agron 82:113–182. https://doi.org/10.1016/S0065-2113(03)82003-5

de Souza MacHado AA, Lau CW, Till J, Kloas W, Lehmann A, Becker R, Rillig MC (2018) Impacts of Microplastics on the Soil Biophysical Environment. Environ Sci Technol 52:9656–9665. https://doi.org/10.1021/acs.est.8b02212

Ding L, Huang D, Ouyang Z, Guo X (2022) The effects of microplastics on soil ecosystem: a review. Curr Opin Environ Sci Heal 26:100344. https://doi.org/10.1016/j.coesh.2022.100344

Dong Y, Gao M, Song Z, Qiu W (2020) Microplastic particles increase arsenic toxicity to rice seedlings. Environ Pollut 259:113892. https://doi.org/10.1016/j.envpol.2019.113892

Duan J, Bolan N, Li Y, Ding S, Atugoda T, Vithanage M, Sarkar B, Tsang DCW, Kirkham MB (2021) Weathering of microplastics and interaction with other coexisting constituents in terrestrial and aquatic environments. Water Res 196:117011. https://doi.org/10.1016/j.watres.2021.117011

Dunne KS, Holden NM, Daly K (2021) Predicting phosphorus sorption isotherm parameters in soil using data of routine laboratory tests. Pedosphere 31:694–704. https://doi.org/10.1016/S1002-0160(21)60012-7

Escudey M, Galindo G, Förster JE, Briceño M, Diaz P, Chang A (2001) Chemical Forms of Phosphorus of Volcanic Ash-Derived Soils in Chile. Commun Soil Sci Plant Anal 32:601–616. https://doi.org/10.1081/CSS-100103895

Escudey M, Forster JE, Galindo G (2004) Relevance of organic matter in some chemical and physical characteristics of volcanic ash-derived soils. Commun Soil Sci Plant Anal 35:781–797. https://doi.org/10.1081/CSS-120030358

Fizir M, Richa A, Touil S, Fermous R, Tahir C, Hassene I, Wei L, Douba H (2024) Comparing Adsorption Properties of Algerian Kaolinite Towards Phosphate with Those of Activated Carbon: Adsorption Experiments, Molecular Modeling and an Initiative Toward Hydroponic Wastewaters Remediation. Water Air Soil Pollut 235:422. https://doi.org/10.1007/s11270-024-07235-w

Gonzalez-Rodriguez S, Fernandez-Marcos ML (2021) Sorption and desorption of vanadate, arsenate and chromate by two volcanic soils of equatorial africa. Soil Syst 5:22. https://doi.org/10.3390/soilsystems5020022

Gu S, Fu B, Ahn JW, Fang B (2021) Mechanism for phosphorus removal from wastewater with fly ash of municipal solid waste

incineration Seoul. Korea J Clean Prod 280:124430. https://doi.org/10.1016/j.jclepro.2020.124430
Hiradate S, Uchida N (2004) Effects of soil organic matter on ph-dependent phosphate sorption by soils. Soil Sci Plant Nutr 50:665–675. https://doi.org/10.1080/00380768.2004.10408523
Horton AA, Walton A, Spurgeon DJ, Lahive E, Svendsen C (2017) Science of the Total Environment Microplastics in freshwater and terrestrial environments: Evaluating the current understanding to identify the knowledge gaps and future research priorities. Sci Total Environ 586:127–141. https://doi.org/10.1016/j.scitotenv.2017.01.190
Hu B, Li Y, Jiang L, Chen X, Wang L, An S, Zhang F (2020) Influence of microplastics occurrence on the adsorption of 17-estradiol in soil. J Hazard Mater 400:123325. https://doi.org/10.1016/j.jhazmat.2020.123325
Jiang XJ, Liu E, Wang T, Zhou T, Xin P (2017) Residual plastic mulch fragments effects on soil physical properties and water flow behavior in the Minqin Oasis northwestern China. Soil Tillage Res 166:100–107. https://doi.org/10.1016/j.still.2016.10.011
Jing K, Min X, Song W, Xu D, Li X (2024) Effect of filling materials on reconstructed soil phosphorus adsorption and desorption in mining area. Soil Tillage Res 235:105895. https://doi.org/10.1016/j.still.2023.105895
Kalam S, Abu-Khamsin SA, Kamal MS, Patil S (2021) Surfactant Adsorption Isotherms: A Review. ACS Omega 6:32342–32348. https://doi.org/10.1021/acsomega.1c04661
Khan TF, Hodson ME (2024) Polyethylene microplastic can adsorb phosphate but is unlikely to limit its availability in soil. Heliyon 10:e23179. https://doi.org/10.1016/j.heliyon.2023.e23179
Kovács RL, Csontos M, Gyöngyösi S, Elek J, Parditka B, Deák G, Kuki Á, Kéki S, Erdélyi Z (2021) Surface characterization of plasma-modified low density polyethylene by attenuated total reflectance fourier-transform infrared (ATR-FTIR) spectroscopy combined with chemometrics. Polym Test 96:107080. https://doi.org/10.1016/j.polymertesting.2021.107080
Li H, Liu L (2022) Short-term effects of polyethene and polypropylene microplastics on soil phosphorus and nitrogen availability. Chemosphere 291:132984. https://doi.org/10.1016/j.chemosphere.2021.132984
Li R, Liu Y, Sheng Y, Xiang Q, Zhou Y, Cizdziel JV (2020) Effect of prothioconazole on the degradation of microplastics derived from mulching plastic film: Apparent change and interaction with heavy metals in soil. Environ Pollut 260:113988. https://doi.org/10.1016/j.envpol.2020.113988
Li M, Jia H, Gao Q, Han S, Yu Y, Sun L (2023) Influence of aged and pristine polyethylene microplastics on bioavailability of three heavy metals in soil: Toxic effects to earthworms (*Eisenia fetida*). Chemosphere 311:136833. https://doi.org/10.1016/j.chemosphere.2022.136833
Li W, Zu B, Ran D, Huang Y, Li J (2021) The adsorption behavior of phosphorus in microplastics in water and soil. J Agro-Environ Sci 40:1758–1764. https://doi.org/10.11654/jaes.2021-0284
Luo H, Chang L, Ju T, Li Y (2024) Factors Influencing the Vertical Migration of Microplastics up and down the Soil Profile. ACS Omega 9:50064–50077. https://doi.org/10.1021/acsomega.4c04083
Ma X, Zhou X, Zhao M, Deng W, Cao Y (2022) Polypropylene microplastics alter the cadmium adsorption capacity on different soil solid fractions. Front Environ Sci Eng 16:1–12. https://doi.org/10.1007/s11783-021-1437-z
Mai H, Thien ND, Dung NT, Valentin C (2023) Impacts of microplastics and heavy metals on the earthworm Eisenia fetida and on soil organic carbon, nitrogen, and phosphorus. Environ Sci Pollut Res 30:64576–64588. https://doi.org/10.1007/s11356-023-27002-4
Malla-Pradhan R, Pradhan BL, Phoungthong K, Joshi TP (2022) Occurrence and Distribution of Microplastics from Nepal's Second Largest Lake. Water Air Soil Pollut 233:423. https://doi.org/10.1007/s11270-022-05896-z
Mezenner NY, Bensmaili A (2009) Kinetics and thermodynamic study of phosphate adsorption on iron hydroxide-eggshell waste. Chem Eng J 147:87–96. https://doi.org/10.1016/j.cej.2008.06.024
Minasny B, Fiantis D, Hairiah K, Van Noordwijk M (2021) Applying volcanic ash to croplands – The untapped natural solution. Soil Secur 3:100006. https://doi.org/10.1016/j.soisec.2021.100006
Murphy J, Riley JP (1962) A modified single solution method for the determination of phosphate in natural waters. Anal Chim Acta 27:31–36. https://doi.org/10.1016/S0003-2670(00)88444-5
Nguyen TK, Li X, Ren L, Huang Y, Zhou JL (2023) Polystyrene and low-density polyethylene pellets are less effective in arsenic adsorption than uncontaminated river sediment. Environ Sci Pollut Res 30:95810–95827. https://doi.org/10.1007/s11356-023-29218-w
Pigna M, Violante A (2003) Adsorption of sulfate and phosphate on Andisols. Commun Soil Sci Plant Anal 34:2099–2113. https://doi.org/10.1081/CSS-120024051
Pinto-Poblete A, Retamal-Salgado J, López MD, Zapata N, Sierra-Almeida A, Schoebitz M (2022) Combined Effect of Microplastics and Cd Alters the Enzymatic Activity of Soil and the Productivity of Strawberry Plants. Plants 11:536. https://doi.org/10.3390/plants11040536
Pizarro C, Escudey M, Gacitua M, Fabris JD (2017) Iron-bearing minerals from soils developing on volcanic materials from southern Chile. Mineralogical characterization supported by Mössbauer spectroscopy. J Soil Sci Plant Nutr 17:341–365. https://doi.org/10.4067/S0718-95162017005000026
Randhawa JS (2023) Advanced analytical techniques for microplastics in the environment: a review. Bull Natl Res Cent 47:174. https://doi.org/10.1186/s42269-023-01148-0
Riveros G, Soria R, Villafuerte A, Gómez P, Ortega R, Miralles I, Schoebitz M (2024) Effects of low-density polyethylene and polyamide microplastics on the microbiological and chemical characteristics of an Andisol. Soil Use Manag 40:e12991. https://doi.org/10.1111/sum.12991
Rusmin R, Sarkar B, Liu Y, McClure S, Naidu R (2015) Structural evolution of chitosan-palygorskite composites and removal of aqueous lead by composite beads. Appl Surf Sci 353:363–375. https://doi.org/10.1016/j.apsusc.2015.06.124
Sadzawka A, Carrasco MA, Grez R, Mora ML, Flores PH, Neaman A (2006) Métodos de análisis recomendados para suelos chilenos. Comisión de Normalización y Acreditación (CNA). Sociedad Chilena de la Ciencia del Suelo. Serie Actas N° 34. Instituto de Investigaciones Agropecuarias (INIA), Centro Regional de Investigación La Platina (INIA La Platina), Santiago Chile
Sarkar B, Mukhopadhyay R, Ramanayaka S, Bolan N, Ok YS (2021) The role of soils in the disposition, sequestration and decontamination of environmental contaminants. Philos Trans R Soc B Biol Sci 376:20200177. https://doi.org/10.1098/rstb.2020.0177
Shao X, Zhang Q, Liang W, Gong K, Fu M, Saif S, Peng C, Zhang W (2023) Polyamide microplastics as better environmental vectors of Cr(VI) in comparison to polyethylene and polypropylene microplastics. Mar Pollut Bull 186:114492. https://doi.org/10.1016/j.marpolbul.2022.114492
Shi L, Hou Y, Chen Z, Bu Y, Zhang X, Shen Z, Chen Y (2022) Impact of polyethylene on soil physicochemical properties and characteristics of sweet potato growth and polyethylene absorption. Chemosphere 302:134734. https://doi.org/10.1016/j.chemosphere.2022.134734
Shirkhorshidi B, Ghanatghestani MD, Moeinpour F, Parvaresh H (2023) The Impacts of Microplastics on Sorption and Desorption Specifications of Iron in Soil. Water Air Soil Pollut 234:379. https://doi.org/10.1007/s11270-023-06395-5

Suazo-Hernández J, Klumpp E, Arancibia-Miranda N, Poblete-Grant P, Jara A, Bol R, Mora M de LL (2021) Describing phosphorus sorption processes on volcanic soil in the presence of copper or silver engineered nanoparticles. Minerals 11:373. https://doi.org/10.3390/min11040373

Suazo-Hernández J, Klumpp E, Arancibia-Miranda N, Jara A, Poblete-Grant P, Sepúlveda P, Bol R, Mora M de la L (2022) Combined effect of soil particle size fractions and engineered nanoparticles on phosphate sorption processes in volcanic soils evaluated by Elovich and Langmuir-Freundlich models. J Soil Sci Plant Nutr. 22:3685–3696. https://doi.org/10.1007/s42729-022-00919-4

Suazo-Hernández J, Urdiales C, Poblete-Grant P, Pesenti H, Cáceres-Jensen L, Sarkar B, Bolan N, de la Luz MM (2023) Effect of particle size of nanoscale zero–valent copper on inorganic phosphorus adsorption–desorption in a volcanic ash soil. Chemosphere 340:139836. https://doi.org/10.1016/j.chemosphere.2023.139836

Tabatabai MA, Bremner JM (1970) an Alkaline Oxidation Method for Determination of Total Sulfur in Soils. Soil Sci Soc Am J 34:62–65. https://doi.org/10.2136/sssaj1970.03615995003400010019x

Vistoso EM, Bolán NS, Theng BKG, de la Mora M, L, (2009) Kinetics of Molybdate and Phosphate Sorption By Some Chilean Andisols. Rev La Cienc Del Suelo y Nutr Veg 9:55–68. https://doi.org/10.4067/s0718-27912009000100005

Vistoso E, Theng BKG, Bolan NS, Parfitt RL, Mora ML (2012) Competitive sorption of molybdate and phosphate in Andisols. J Soil Sci Plant Nutr 12:59–72. https://doi.org/10.4067/s0718-95162012000100006

Vithanage M, Ramanayaka S, Hasinthara S, Navaratne A (2021) Compost as a carrier for microplastics and plastic-bound toxic metals into agroecosystems. Curr Opin Environ Sci Heal. 24:100297.https://doi.org/10.1016/j.coesh.2021.100297

Wang F, Zhang M, Sha W, Wang Y, Hao H, Dou Y, Li Y (2020) Sorption behavior and mechanisms of organic contaminants to nano and microplastics. Molecules 25:1827. https://doi.org/10.3390/molecules25081827

Wang F, Wang Q, Adams CA, Sun Y, Zhang S (2022) Effects of microplastics on soil properties: Current knowledge and future perspectives. J Hazard Mater 424:127531. https://doi.org/10.1016/j.jhazmat.2021.127531

Zhang S, Han B, Sun Y, Wang F (2020a) Microplastics influence the adsorption and desorption characteristics of Cd in an agricultural soil. J Hazard Mater 388:121775. https://doi.org/10.1016/j.jhazmat.2019.121775

Zhang W, Zhang L, Hua T, Li Y, Zhou X, Wang W, You Z, Wang H, Li M (2020b) The mechanism for adsorption of Cr(VI) ions by PE microplastics in ternary system of natural water environment. Environ Pollut 257:113440. https://doi.org/10.1016/j.envpol.2019.113440

Zhang X, Li Y, Ouyang D, Lei J, Tan Q, Xie L, Li Z, Liu T, Xiao Y, Farooq TH, Wu X, Chen L, Yan W (2021) Systematical review of interactions between microplastics and microorganisms in the soil environment. J Hazard Mater 418:126288. https://doi.org/10.1016/j.jhazmat.2021.126288

Zhao T, Lozano YM, Rillig MC (2021) Microplastics Increase Soil pH and Decrease Microbial Activities as a Function of Microplastic Shape, Polymer Type, and Exposure Time. Front Environ Sci 9:675803. https://doi.org/10.3389/fenvs.2021.675803

Zhao D, Qiu S kai, Li M meng, Luo Y, Zhang L sheng, Feng M han, Yuan M yao, Zhang K qiang, Wang F (2022) Modified biochar improves the storage capacity and adsorption affinity of organic phosphorus in soil. Environ Res 205:112455. https://doi.org/10.1016/j.envres.2021.112455

Zhou Y, Yang Y, Liu G, He G, Liu W (2020) Adsorption mechanism of cadmium on microplastics and their desorption behavior in sediment and gut environments: The roles of water pH, lead ions, natural organic matter and phenanthrene. Water Res 184:116209. https://doi.org/10.1016/j.watres.2020.116209